Journal of Sound and Vibration 329 (2010) 2751–2767

Contents lists available at ScienceDirect

Journal of Sound and Vibration

journal homepage: www.elsevier.com/locate/jsvi

Two-mode vibration control of a beam using nonlinear synchronized switching damping based on the maximization of converted energy

Hongli Ji [a], Jinhao Qiu [a,*], Kongjun Zhu [a], Adrien Badel [b]

[a] Aeronautic Science Key Laboratory for Smart Materials and Structures, College of Aerospace Engineering, Nanjing University of Aeronautics and Astronautics, #29 Yudao Street, Nanjing 210016, China

[b] Laboratory of Systems and Materials for Mechatronics, Polytech'Savoie, Savoie University, BP 80439, 74944 Annecy le Vieux Cedex, France

ARTICLE INFO

Article history:
Received 10 May 2009
Received in revised form
8 January 2010
Accepted 11 January 2010
Handling Editor: D.J. Wagg
Available online 24 February 2010

ABSTRACT

In this paper, a new switch control strategy based on an energy threshold is proposed for the synchronized switch damping techniques in multimode control. This strategy is derived from the total converted energy of a synchronized switch damping (SSD) system in a given time window. Using the new strategy the voltage is inverted only at those extrema where the effective distance, which is proportional to the converted energy between two neighboring extrema, exceeds the threshold. The new switch control strategy is used in both the synchronized switch damping on inductor (SSDI) technique and the synchronized switch damping on voltage source (SSDV) technique, which are applied to the two-mode control of a composite beam. Their control performances are compared with those of the single-mode control and those of classical SSDI and SSDV techniques in two-mode control. The experimental results show that voltage inversion is prevented at some of the displacement extrema to increase the total converted energy, and exhibit better global damping effect than classical SSDI and classical SSDV, respectively. In single mode, the best control performance is achieved when the voltage is inverted at every extremum. But in multimodal control, the total converted energy in a given time window is increased and the control performance is improved when some extrema are skipped.

1. Introduction

Piezoelectric element is one of the most attractive functional materials for smart structures because of good mechanical–electrical coupling characteristics, frequency response and reliability. The methods of vibration control using piezoelectric element can be divided into three categories: passive, active and semi-active [1–3]. In the past decade, semi-active vibration control methods based on switching shunt circuits have attracted the attention of many researchers in this field [4–7]. The switching techniques can be divided into two types: state-based switching technique and synchronized switching technique. The state-based switching technique is basically applicable to multimode control, but it requires powerful digital signal processing system for estimation of state variables [7]. The synchronized switching damping (SSD) techniques have several advantages compared with other methods: the control system is very simple and compact [8–10]. The shunt circuit does not require complicated digital signal processing system, nor bulky amplifier and external power sources. Moreover, the shunt circuit configuration does not require a parametric model of the vibrating structure for design

* Corresponding author. Tel./fax: +86 25 84891123.
E-mail address: qiu@nuaa.edu.cn (J. Qiu).

0022-460X/$ - see front matter © 2010 Elsevier Ltd. All rights reserved.
doi:10.1016/j.jsv.2010.01.012

purposes, and is correspondingly easier to implement. In addition, the control performance is not sensitive to the variation of the parameters of the system.

The principle of SSD techniques is to invert the voltage on the piezoelectric patches so that a phase shift is induced on the voltage relative to the displacement. The phase shift leads to a net conversion of the mechanical energy of vibration to the electrical energy stored on the piezoelectric patch in each vibration cycle. The electrical energy is then dissipated in the shunt circuit. Several techniques of SSD have been developed, including SSDS (synchronized switch damping on short circuit) [10], SSDI (synchronized switch damping on inductor) [8], SSDV (synchronized switch damping with voltage source) [11,12]. In all the SSD techniques, the switch is controlled by the same strategy, which inverts the voltage at each extremum of displacement to guarantee that the force generated by the voltage is in opposite direction with the vibration velocity. For single-mode vibration control, this algorithm has been proven to be effective. However, in multimodal vibration, the number of extrema in the displacement curve may increase drastically due to the extrema of different modes so that this strategy is no longer efficient because over-frequent switching may reduce the voltage on the piezoelectric patch. Hence design of new switch control strategy is an important issue for the application of SSD techniques in multimode vibration control.

Several research works on application of the SSD technique in multimodal vibration control have been reported. Corr and Clark [13] experimented with SSDI or pulse switching in the case of a multimodal vibration. The proposed technique consists of selecting the modes to be controlled using numerical filtering techniques. Filtering devices were used to select modes to be controlled, but filtering inevitably leads to time delay of switching actions that result in a lack of effectiveness. Niederberger [14] used a hybrid system optimal control approach to derive the optimal switching laws of electronic shunt circuits for mechanical vibration suppression of a beam. Simulation results showed that the switching laws are also effective for two-mode control. Guyomar et al. [15] proposed a novel multimodal control law for the SSD technique based on a probabilistic approach and achieved good control performance, but the control performance was checked only by simulation. The amount of calculation of this method is relatively larger because the probabilistic distribution of displacement in a given time window needs to be calculated for switch control. Following the probabilistic approach, an enhanced control strategy for random vibration control based on statistics was developed by Guyomar [16]. A significant decrease in vibration energy was demonstrated experimentally and theoretically in the case of a clamped beam excited by random noise. In the case of multimodal vibration, all of the modes were controlled. The authors of this paper proposed a simple switch control strategy based on a displacement threshold in the former study [17]. The experimental results exhibited good performance of the simple switch control strategy in multimode vibration control of a composite beam with much less CPU load of computation.

In this study a new switch control strategy to maximize of the converted energy is developed to address the problem of SSD technique in multimodal vibration control. For simplicity, the control of two-mode vibration is considered in this study. The new switch control strategy is based on the converted energy in a given time window and an energy threshold is set for the converted energy between two neighboring switching points to increase the total converted energy. The new strategy is applied to the two-mode vibration control of a composite beam and the control results are compared with those of the SSDI and SSDV using the classical switch. In Section 2, multimodal modeling of a clamped-free beam with piezoelectric elements is presented. The switching strategy is discussed in detail in Section 3. The experimental system is introduced in Section 4, and the experimental results of multimodal vibration control and their discussions are given in Section 5.

2. The mechanical model of the beam

The structure used in the experiment is a cantilever GFRP (glass fiber reinforced plastics) composite beam with two embedded piezoelectric patches which are close to the end of clamped beam, as shown in Fig. 1. The composite beam was made from four layers of GFRP prepreg and the piezoelectric patch is laminated in the following order: 0°/90°/90°/PZT/0°,

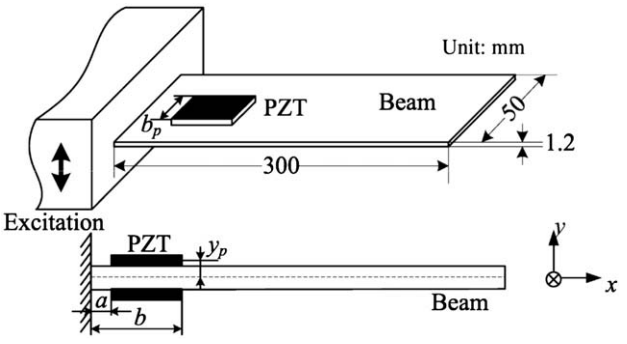

Fig. 1. Schematic representation of the system.

where 0° is the length direction of the beam. The beam is 300 mm long, 50 mm wide and 1.2 mm thick and its properties are given in Table 1. The dimension of piezoelectric patches is a square of 30 mm × 30 mm and 0.2 mm thick. They are polarized in the thickness directions which are perpendicular to the beam and their properties are given in Table 2. The two piezoelectric elements are electrically connected in parallel.

The Euler–Bernoulli assumptions are used for the vibration analysis of the beam. It is also assumed that the beam is homogenous in material properties and uniform in geometry, that is, the influence of embedded piezoelectric patch on the stiffness is neglected. If the deflection of the beam is denoted by $u(x, t)$, the equation of motion can be expressed in the following form:

$$\rho A\frac{\partial^2 u(x,t)}{\partial t^2}+c\frac{\partial u(x,t)}{\partial t}+EI\frac{\partial^4 u(x,t)}{\partial x^4}=f(x,t), \tag{1}$$

where $\rho(x)$ is the mass per unit length, A is the cross-sectional area, c is the damping coefficient, E is the Young's modulus, I is the moment of inertia, and $f(x, t)$ is the distributed external force. The force $f(x, t)$ includes two parts: the force for excitation, $f_e(x, t)$, and the one generated by the piezoelectric actuators for control, $f_p(x, t)$. After modal analysis, the natural frequencies and modal functions can be obtained. The natural frequencies of the first and second modes are 11 and 68.8 Hz, respectively.

The deflection $u(x, t)$ of the beam under external excitation can be written as the summation of modal coordinates in the beam and the eigenmode functions. This is shown as

$$u(x,t)=\sum_{i=1}^{\infty}\phi_i(x)u_i(t), \tag{2}$$

where $\phi_i(x)$ is the ith modal function and $u_i(t)$ is the ith modal coordinate. Substituting (2) into (1) and considering the orthogonality of modal functions, the following equation can be obtained:

$$M_i\ddot{u}_i+C_i\dot{u}_i+K_{Ei}u_i=F_{ei}+F_{pi}, \tag{3}$$

where M_i is the modal mass, C_i is the modal damping factor, K_{Ei} is the modal stiffness, F_{ei} is the modal force of excitation, and F_{pi} is modal force generated by the piezoelectric patch. The system parameters in Eq. (3) can be expressed as

$$M_i=\int_0^L\rho A\phi_i^2(x)\,dx,\quad K_i=\int_0^L EI\phi''^2_i(x)\,dx=\omega_i^2\int_0^L\rho A\phi_i^2(x)\,dx,\quad F_{ei}=\int_0^L f_e(x,t)\phi_i(x)\,dx,\quad F_{pi}=\int_0^L f_p(x,t)\phi_i(x)\,dx. \tag{4}$$

The damping coefficient C_i must be estimated experimentally. In this study the damping coefficient of each mode was calculated from the decaying time response of free vibration of that mode. The distributed force $f_p(x, t)$ is proportional to the voltage on the piezoelectric patch and can be expressed as

$$f_p(x,t)=-2y_pb_pe_{31}V[\delta'(x-b)-\delta'(x-a)], \tag{5}$$

where y_p is the distance from the mid-plane of the piezoelectric patch to the mid-plane of the beam, b_p is the width of the piezoelectric patches, e_{31} is the piezoelectric constant, δ is the Dirac delta function and a and b are the x coordinates of the piezoelectric patches. The system in Eq. (3) is illustrated in Fig. 1. Substitution of Eq. (5) into the expression of F_{pi} in

Table 1
Material properties of the composite beam.

	GFRP
Elastic modulus E_1	$1.65\times10^{+10}$ (N/m^2)
Elastic modulus E_2	$3.52\times10^{+10}$ (N/m^2)
Poisson ratio	0.109
Shear modulus	$1.25\times10^{+10}$ (N/m^2)
Density	1900 (kg/m^3)
Thickness	1.2×10^{3} (m)

Table 2
Material properties of the piezoelectric patch.

	PZT
Elastic modulus	$59\times10^{+9}$ (N/m^2)
Poisson ratio	0.345
Density	7400 (kg/m^3)
Thickness	2×10^{4} (m)
Piezoelectric constant d_{31}	260×10^{12} (m/V)
Capacitance C_p	141×10^{9} (F)

Eq. (4) gives

$$F_{pi} = -a_{iV}, \tag{6}$$

where

$$\alpha_i = 2y_p b_p e_{31}[\phi_i'(x-b) - \phi_i'(x-a)]. \tag{7}$$

Eq. (6) indicates that the modal force is proportional to the voltage V on the piezoelectric patch. If the displacement sensor is used to measure the displacement of the beam at $x=x_s$, output value is

$$u = u(x_s, t) = \sum_{i=1}^{\infty} \phi_i(x_s) u_i(t). \tag{8}$$

The above equation means that the measured output is linear combination of the modal coordinates u_i. Although almost all engineering structures are continuum, their vibration can be expressed as the superposition of modal vibration using modal coordinate as shown in Eq. (8). At the resonance frequency of specific mode, the system can be simplified as single-degree-of freedom and expressed by an ordinary differential equation (3).

In this study, as the first step to the general multimode control, only the resonant vibrations of the first and the second natural modes are considered. It is assumed that the amplitudes of the first mode and the second mode are dominant and the higher-order modes can be neglected. The following energy equation of the system with two modes considered is obtained by multiplying both sides of Eq. (3) by the velocity, integrating over the time variable and taking summation.

$$\int (F_{e1}\dot{u}_1 + F_{e2}\dot{u}_2)\,\mathrm{d}t = \frac{1}{2}(M_1\dot{u}_1^2 + M_2\dot{u}_2^2) + \frac{1}{2}(K_{E1}u_1^2 + K_{E2}u_2^2) + \int (C_1\dot{u}_1^2 + C_2\dot{u}_2^2)\,\mathrm{d}t + \int (\alpha_1\dot{u}_1 + \alpha_2\dot{u}_2)V\,\mathrm{d}t. \tag{9}$$

The provided energy is divided into kinetic energy, potential elastic energy, mechanical losses, and transferred energy. In the steady state, the sum of the kinetic energy and the elastic energy can be considered to be constant for each mode. Hence the input energy, which increases with the time of integration in Eq. (9), is balanced by the mechanical losses and the transferred energy. The transferred energy corresponds to the part of the mechanical energy which is converted into electrical energy through the action of modal force and dissipated in the shunt circuit. Maximizing this energy is equivalent to minimizing the mechanical energy in the structure if the energy provided by the external excitation is the same (Fig. 2).

3. Control strategy

Fig. 3 shows the relationship between the displacement, velocity and voltage on the piezoelectric element in a vibration system. Without switching action, the voltage is proportional to the displacement [15]. The converted energy expressed by the last term in Eq. (9) is zero in a period of mechanical vibration. In the SSD techniques, a phase shift is induced in the voltage on the piezoelectric element and consequently a net energy conversion is generated by the switching actions of the shunt circuit. In the several variations of SSD, the SSDI technique is relatively efficient and does not need external energy in driving the piezoelectric element so that it can be used as a good benchmark method in evaluating the efficiency of a switching strategy.

In SSDI technique the voltage on the piezoelectric patch is inverted at the extrema of the vibration displacement by the switch circuit as shown in Fig. 3. The objective of a control strategy is to maximize the converted energy. The voltage on the piezoelectric element in the steady state of SSDI control can be decomposed into two components as illustrated in Fig. 4, a rectangular signal due to switching action and a signal that is an image of the strain variation. That is, the voltage on the piezoelectric element can be expressed in the following form:

$$V = V_{sw} + V_{st}, \tag{10}$$

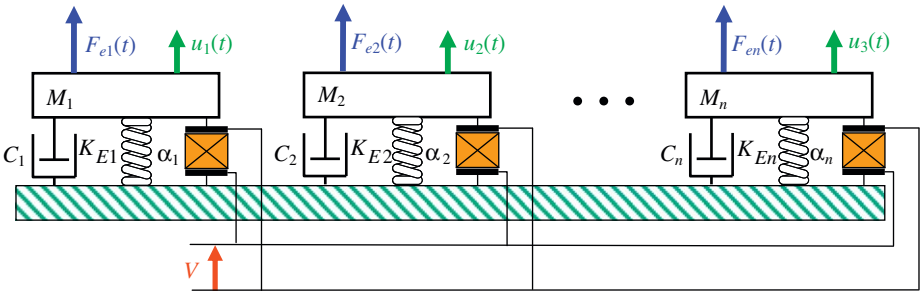

Fig. 2. Diagram of the multimode electromechanical model.

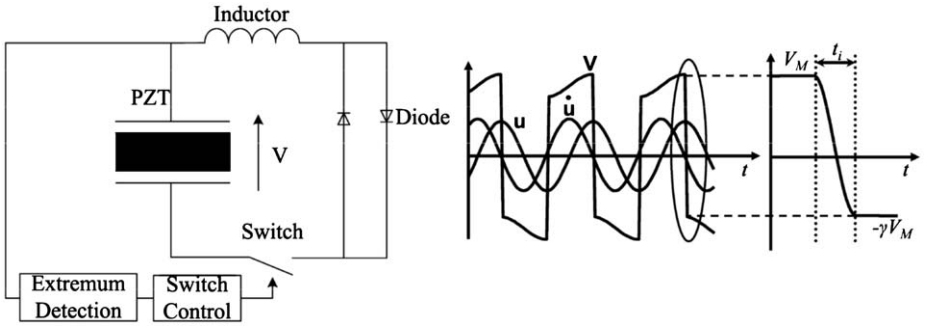

Fig. 3. Schematic diagram of a SSDI control system.

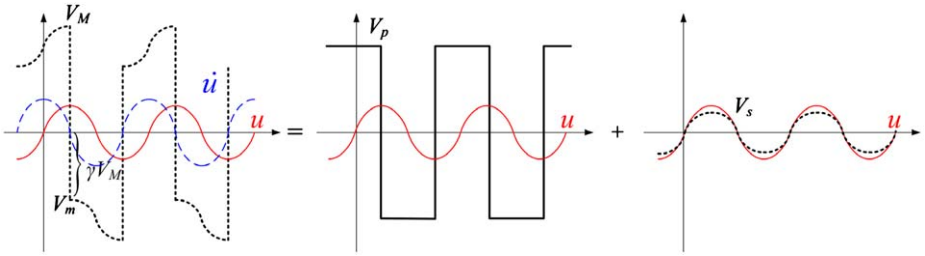

Fig. 4. Decomposition of the voltage signal in SSD techniques.

where V_{sw} is the rectangular single and V_{st} is generated by strain variation. As shown in [12,17], the voltage generated by strain can be written as

$$V_{st} = \frac{1}{C_p}(\alpha_1 u_1 + \alpha_2 u_2), \tag{11}$$

where C_p is the capacitance of the piezoelectric element and defined as

$$C_p = \frac{\varepsilon_{33} b_p (b-a)}{h_p}, \tag{12}$$

where h_p is the thickness of the piezoelectric element. The converted energy for the ith mode can be expressed as

$$\int \alpha_i (V_{sw} + V_{st}) \dot{u}_i \, dt = \int \alpha_i V_{sw} \dot{u}_i \, dt + \int \alpha_i V_{st} \dot{u}_i \, dt = \int \alpha_i V_{sw} \, du_i + \int \alpha_i V_{st} \, du_i. \tag{13}$$

In the case of single-mode control, it has been proved that $\int \alpha_i V_{st} \, du_i = \int \alpha_i^2 u_i \, du_i$ is zero in a period of mechanical vibration [12,18]. In multimode control, this term becomes more complicated because different modes have different periods and there are coupling effects between different modes. However, physically this term corresponds to the energy that is converted reciprocally between mechanical and electrical in different phases of vibration and does not contribute to vibration damping so that it does not need to be considered.

Mathematically, it can be proved that the value of $\int \alpha_i V_{st} \, du_i$ is relatively small compared to $\int \alpha_i V_{sw} \, du_i$ for a large time window. Without loss of generality, assuming that the index i in Eq. (13) is 1 and the considered duration of time is $(0, T)$, the second term can be expressed as

$$\int_{u_1(0)}^{u_1(T)} \alpha_1 V_{st} \, du_1 = \frac{\alpha_1}{C_p} \left(\int_{u_1(0)}^{u_1(T)} \alpha_1 u_1 \, du_1 + \int_{u_1(0)}^{u_1(T)} \alpha_2 u_2 \, du_1 \right). \tag{14}$$

Since u_1 and u_2 are modal coordinates, they can be expressed as

$$u_1 = u_{1M} \sin(\omega_1 t - \varphi_1), \quad u_2 = u_{2M} \sin(\omega_2 t - \varphi_2),$$

where u_{1M} and u_{2M} are the amplitudes, ω_1 and ω_2 are the angular frequencies, and φ_1 and φ_2 are the initial phase of the modes, respectively. From the properties of triangular functions, the first integration on the right-hand side of the above equation is bounded by $\alpha_1^2 u_{1M}^2/(2C_p)$ and the second term is bounded by $\alpha_1 \alpha_2 u_{1M} u_{2M}/C_p$ independent of the integration duration. If sufficiently long duration of time is considered, the average converted energy in each cycle of vibration is negligible. Hence the objective of optimizing switching algorithm is to maximize $\int \alpha_i V_{sw} \, du_i$ in a given duration of time. As it will be shown later the term $\int \alpha_i V_{sw} \, du_i$ increases with the considered duration of time.

In the following derivation, $\int \alpha_i V_{st}\,du_i$ will not be considered. Moreover, in the steady state the magnitude of V_{sw} is almost constant, but its sign is reversed at each switching point. For two-mode control, the converted energy can be written as

$$\begin{aligned}\int (F_{e1}\dot{u}_1+F_{e2}\dot{u}_2)\,dt &= \int (C_1\dot{u}_1^2+C_2\dot{u}_2^2)\,dt+\int (\alpha_1 V_{sw}\,du_1+\alpha_2 V_{sw}\,du_2)\\ &= \int (C_1\dot{u}_1^2+C_2\dot{u}_2^2)\,dt+\int \alpha V_{sw}\,d(\tilde{\alpha}_1 u_1+\tilde{\alpha}_2 u_2)\\ &= \int (C_1\dot{u}_1^2+C_2\dot{u}_2^2)\,dt+\int \alpha V_{sw}\,d\tilde{u}, \end{aligned} \tag{15}$$

where α is an arbitrary voltage constant used to normalize α_1 and α_2, and

$$\tilde{\alpha}_1=\alpha_1/\alpha,\quad \tilde{\alpha}_2=\alpha_2/\alpha,\quad \tilde{u}=\tilde{\alpha}_1 u_1+\tilde{\alpha}_2 u_2, \tag{16}$$

$\tilde{u}$ is a virtual displacement, which is usually difficult to measure in a physical system. The above normalization is performed just to keep the final term of Eq. (15) in the same form as that in the single-mode control. On the other hand, in order to obtain damping effect, it is necessary to keep the sign of V_{st} the same as that of the velocity $\dot{u}$, as shown in Fig. 4, so that the electrical energy is converted to mechanical energy all the time. It means that the information of $\tilde{u}$ is necessary for the switch control. In order to solve this problem, the measured displacement in Eq. (8) rewritten as

$$u_s=\phi_1(x_s)u_1+\phi_2(x_s)u_2 \tag{17}$$

in the two-mode case. If an appropriate measuring point is chosen so that

$$\phi_1(x_s):\phi_2(x_s)=\tilde{\alpha}_1:\tilde{\alpha}_2=\alpha_1:\alpha_2, \tag{18}$$

it is possible to make the measured displacement and virtual displacement proportional, that is,

$$\tilde{u}=\kappa u_s=\kappa[\phi_1(x_s)u_1+\phi_2(x_s)u_2], \tag{19}$$

where κ is a constant. Hence the extrema of u_s can be used for switch control. In this study, the measurement point is chosen to satisfy the condition (18) so that the measured displacement can be used in the switch control. When the number of considered modes is more than two, this kind of measurement will be difficult to find in a real structure. However, this problem can be solved by a piezoelectric sensor collocated with the piezoelectric actuator for semi-active control. For the collocated piezoelectric sensor, its output voltage is given by Eq. (13), which is proportional to the virtual displacement.

In order to have better understanding of the complexity in multimode control, the converted energy is written in the following form:

$$\int_{u(t_j)}^{u(t_{j+1})} \alpha V_{sw}\,du=\int_{u(t_j)}^{u(t_{j+1})} \alpha_1 V_{sw}\,du_1+\int_{u(t_j)}^{u(t_{j+1})} \alpha_2 V_{sw}\,du_2, \tag{20}$$

where t_j and t_{j+1} are the times of the jth and $(j+1)$th switching point. The meaning of each term is straightforward. From Eq. (20), the following switch control rule can be obtained.

Switch control rule 1: The condition to obtain net converted energy between two switching points is to make V_{sw} and $\dot{u}$ have the same sign.

The above rule is the same as inverting voltage at the displacement extrema. However, even if the above condition is satisfied, the V_{sw} do not always have the same sign as each $\dot{u}_i$ ($i=1, 2$). Because the two modes have different frequencies, $\dot{u}_1$ and $\dot{u}_2$ may have opposite sign so that V_{sw} can only take the same sign with one of the two velocities. In that case one mode is damped, and the other mode is excited. This makes it difficult to design an optimal control strategy. The simplest switch control scheme is to switch the voltage at each extremum, which is the same as that in the single-mode control. However, due to the limitation of voltage inversion factor, this scheme has been proved in the experiment to be not optimal for multimode control [15–17].

In order to investigate the energy conversion efficiency, the total converted energy in a given time window $(0, T)$ is considered. This time window is much longer than the periods of both modes so that multiple cycles of vibration are contained in it. The total number of extrema is N and the total times of switching action, which takes place at some extrema of the resultant displacement in this time window, is assumed to be $2n$, satisfying $2n<N$. The converted energy is

$$\begin{aligned}\int_0^T \alpha V_{sw}\dot{u}\,dt &= \alpha|V_{sw}|\int_0^T \mathrm{sign}(V_{sw})\dot{u}\,dt\\ &= \alpha|V_{sw}|\sum_{j=1}^{2n}\mathrm{sign}(V_{sw})\int_{u(t_{j-1})}^{u(t_j)} du\\ &= \alpha|V_{sw}|\sum_{j=1}^{2n}\mathrm{sign}(V_{sw})[u(t_j)-u(t_{j-1})]\end{aligned}$$

$$= \alpha |V_{sw}| \sum_{j=1}^{2n} |u(t_j) - u(t_{j-1})|$$
$$= \alpha |V_{sw}| \sum_{j=1}^{2n} |\Delta u_j|$$
$$= \alpha |V_{sw}| 2n \overline{|\Delta u_j|}, \tag{21}$$

where $|V_{sw}|$ is considered to be constant at the steady state, t_j (j=0,1, …, $2n$) are switching time so that V_{sw} does not change sign between t_{j-1} and t_j, Δu_j is the displacement of the beam between t_{j-1} and t_j, and $\overline{|\Delta u_j|}$ is the average effective distance between the neighboring points.

The relation between the voltage before inversion, $V_{M,j-1}$, and the voltage after inversion $V_{m,j}$ can be expressed in the following form:

$$V_{m,j} = \gamma V_{M,j-1}, \tag{22}$$

where γ is the inversion coefficient, which is between 0 and 1 between the voltages are expressed in their absolute values [12]. On the other hand, the voltage $V_{m,j}$ is increased to $V_{M,j}$ by the displacement of vibration before the next switching point. Their relation can be expressed as

$$V_{M,j} = V_{m,j} + \frac{\alpha}{C_0} |\Delta u_j|, \tag{23}$$

where C_0 is the capacitance of the piezoelectric patch. Summation of Eq. (22) with respect to index j and considering Eq. (23) gives

$$\sum_{j=1}^{2n} V_{M,j} = \frac{\alpha/C_0}{1-\gamma} \sum_{j=1}^{2n} |\Delta u_j|. \tag{24}$$

It has been assumed that $V_{M,0} = V_{M,2n}$ in the derivation of the above equation. Since $|\Delta u_j|$ varies with j, neither $V_{M,j}$ or $V_{m,j}$ is constant. However as an approximation, it is assumed that $V_{M,j}$ and $V_{m,j}$ are constant in the steady state. This assumption may not hold for each cycle of vibration, but statistically the error caused by the assumption is relatively small for a certain time window. The amplitude of the rectangular wave is

$$|V_{sw}| = \frac{1}{2}(V_M + V_m) = \frac{1+\gamma}{2} V_M$$
$$= \frac{1+\gamma}{2} \frac{1}{2n} \frac{\alpha/C_0}{1-\gamma} \sum_{j=1}^{2n} |\Delta u_j|$$
$$= \frac{1+\gamma}{1-\gamma} \frac{\alpha}{2C_0} \frac{1}{2n} \sum_{j=1}^{2n} |\Delta u_j|$$
$$= \frac{1+\gamma}{1-\gamma} \frac{\alpha}{2C_0} \overline{|\Delta u_j|}. \tag{25}$$

Substitution of Eq. (25) into (21) gives

$$\int_0^T \alpha V_{sw} \, du = \frac{1+\gamma}{1-\gamma} \frac{\alpha^2}{2C_0} 2n \overline{|\Delta u_j|}^2. \tag{26}$$

Eq. (26) indicates that the converted energy $\int_0^T \alpha V_{sw} \, du$ depends on both the number of switching action $2n$ and the average effective distance $\overline{|\Delta u_j|}$, but it is more sensitive to the later because it is squared in the equation.

According to Eq. (26), the converted energy can be increased by increasing the number of switching action $2n$ and average effective distance $\overline{|\Delta u_j|}$. However it is impossible to increase both $2n$ and $\overline{|\Delta u_j|}$ simultaneously, and a tradeoff must be made between them. Since the voltage is switched at displacement extrema, the maximum value of $2n$ equals the number of displacement extrema, N, in the time window $(0, T)$. However experimental results exhibit that optimal control performance is not achieved at $2n$=N, but at $2n < N$ by skipping some displacement extrema [15–17]. This means that decreasing $2n$ can increase $\overline{|\Delta u_j|}$, consequently increase converted energy. The following is an example to explain how decrease of $2n$ can increase $|\Delta u_j|$.

As shown in Fig. 5, after the voltage is inverted at the displacement minimum at t_{j-1}, the next switching point is the displacement maximum at t'_j if a classical switch is used. However, the effective displacement $|\Delta u'_j| = u(t'_j) - u(t_{j-1})$, which is difference of displacements at the two extrema and is directly proportional to the converted energy between the two switching points, is relatively small. If the extremum at t'_j is skipped and the voltage is inverted at t_j, the effective distance becomes $|\Delta u'_j| = u(t_j) - u(t_{j-1})$, which is greater than $|\Delta u'_j|$. Consequently the average effective distance $\overline{|\Delta u_j|}$ can be increased. This means that if some of the extrema are skipped the total converted energy can be increased.

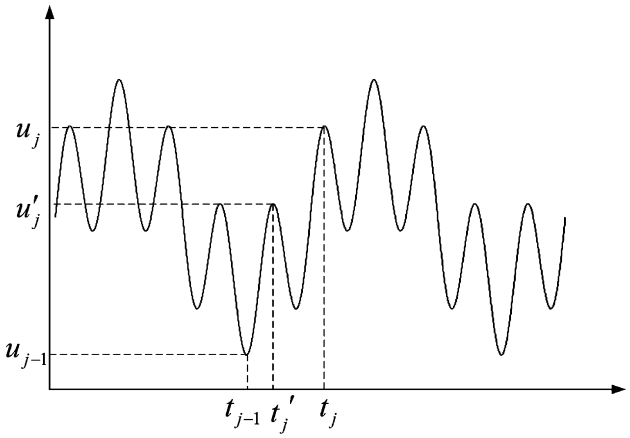

Fig. 5. Schematic view of the switching strategy.

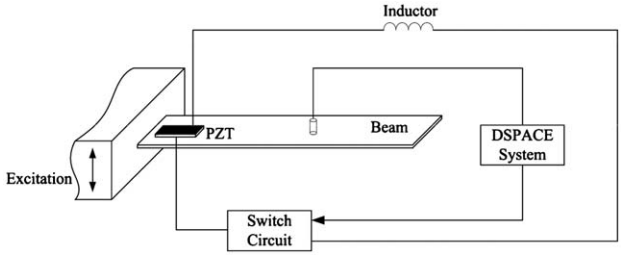

Fig. 6. Experimental setup.

Based on the above discussion, it can be concluded that in order to increase the converted energy a threshold can be set on the effective distance $|\Delta u_j|$ to control the switch. The switch control rule can be written as:

Switch control rule 2: If $|\Delta u_j| \geq \Delta u_{cr}$, the voltage is inverted at the extremum; otherwise, the extremum is skipped, where Δu_{cr} is a threshold.

Since $|\alpha V_{sw} \Delta u_j|$ is the converted energy between two switching points, this rule is called energy-based rule. In order to use the second switch control rule, Δu_{cr} must be determined first. Since the displacement depends on many factors such as measurement position, excitation level, etc., no pre-determined value of Δu_{cr} can be set. Hence in the implementation of the second rule, Δu_{cr} is set to an average value of preceding m effective distances multiplied by a coefficient, that is,

$$\Delta u_{cr,j} = \beta \sum_{k=1}^{m} |\Delta u_{j-k}|, \tag{27}$$

where $0 < \beta < 1$. The optimal value of β can be determined only by experience. In this study test running of control experiments was performed under different conditions and the results indicate that the range of optimal β is from 0.5 to 0.7. It should be noticed that the new switch control strategy is the same as the classical switch control strategy in single-mode control.

4. Experimental setup for control

The experimental setup is shown in Fig. 6. One end of the beam is clamped and the other is free. The clamped condition was achieved by putting one end of the composite plate between two aluminum blocks which are bonded together tightly with two bolts. The first two resonance modes are considered. The piezoelectric patches are located at the surface of the clamped end, where the maximum strain of the first two modes is induced. The clamped end is mounted on a mini-shaker, which is used to excite the vibration of the beam. The natural frequencies of the first two modes of the beam were estimated experimentally from the frequency response of the beam by sweeping the excitation frequency from 5 Hz to 80 Hz. The estimated values of the first two natural frequencies are 11 and 68.8 Hz, respectively. In order that Eq. (18) is satisfied, the displacement sensor is putted at x=145 mm, not the free end the beam, to measure the vibration displacement. The displacement signal is used to generate switching signal. As the number of mode to be controlled increases, the sensor point may become more difficult to choose so that more sophisticated identification system will be necessary.

The control approach is implemented in a DSP environment based on the dSPACE board DS1103. The displacement signal from the laser sensor is converted to digital and sent to the DSP system. The extrema on the displacement signal are detected by comparing three consecutive points. After an extremum is found, the effective distance Δu_j is calculated. Based on switch control rule 2, if the $|\Delta u_j| \geq \Delta u_{\mathrm{cr},j}$ is satisfied, the voltage is inverted. Otherwise, the extremum is skipped. The value of β was set to 0.6 in the experiment.

In the control experiment, the new switch control strategy based on the energy threshold is applied to the SSDI approach and its performance is compared with that of the classical SSDI, in which the voltage on the piezoelectric patch is inverted at each extremum. The new switch control strategy is also combined with the adaptive SSDV based on LMS algorithm, which was proposed by the author in the former study [18], and its performance is compared with that of the classical SSDV, in which the voltage source is optimized manually.

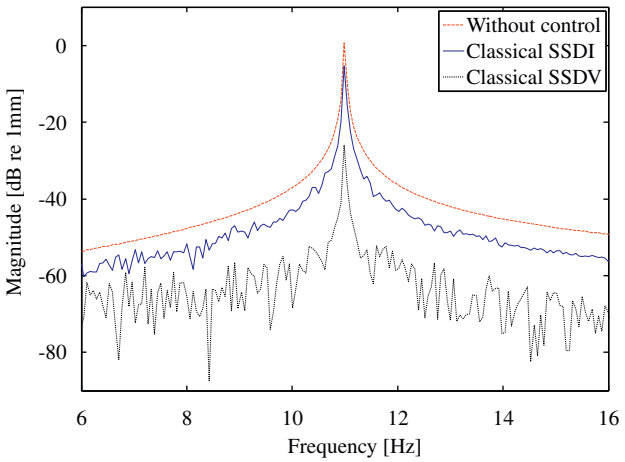

Fig. 7. Control performances of the first mode with classical SSDI and classical SSDV in single-mode control.

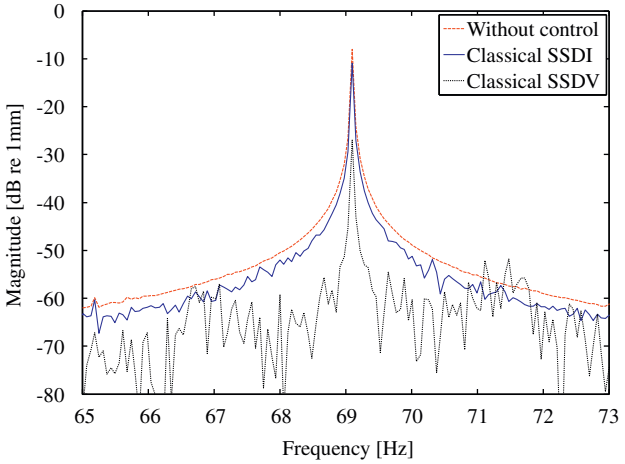

Fig. 8. Control performances of the second mode with classical SSDI and classical SSDV in single-mode control.

Table 3
The control performances of SSDI and SSDV in single-mode control.

Frequency (Hz)	Peak value without control (dB)	Peak value (upper) and reduction (lower) with classical SSDI (dB)	Peak value (upper) and reduction (lower) with classical SSDV (dB)
11	0.8	−5.2	−25.9
		−6	−26.7
69.1	−8	−11	−27
		−3	−19

5. Results and discussion

In order to evaluate the control performance of the new method in multimodal control, the single-mode control and two-mode control of the beam using the classical SSDI and classical SSDV are carried out first. Their results are used in the comparison with the results of the new control method. For easy comparison of their control performance, the spectrum of

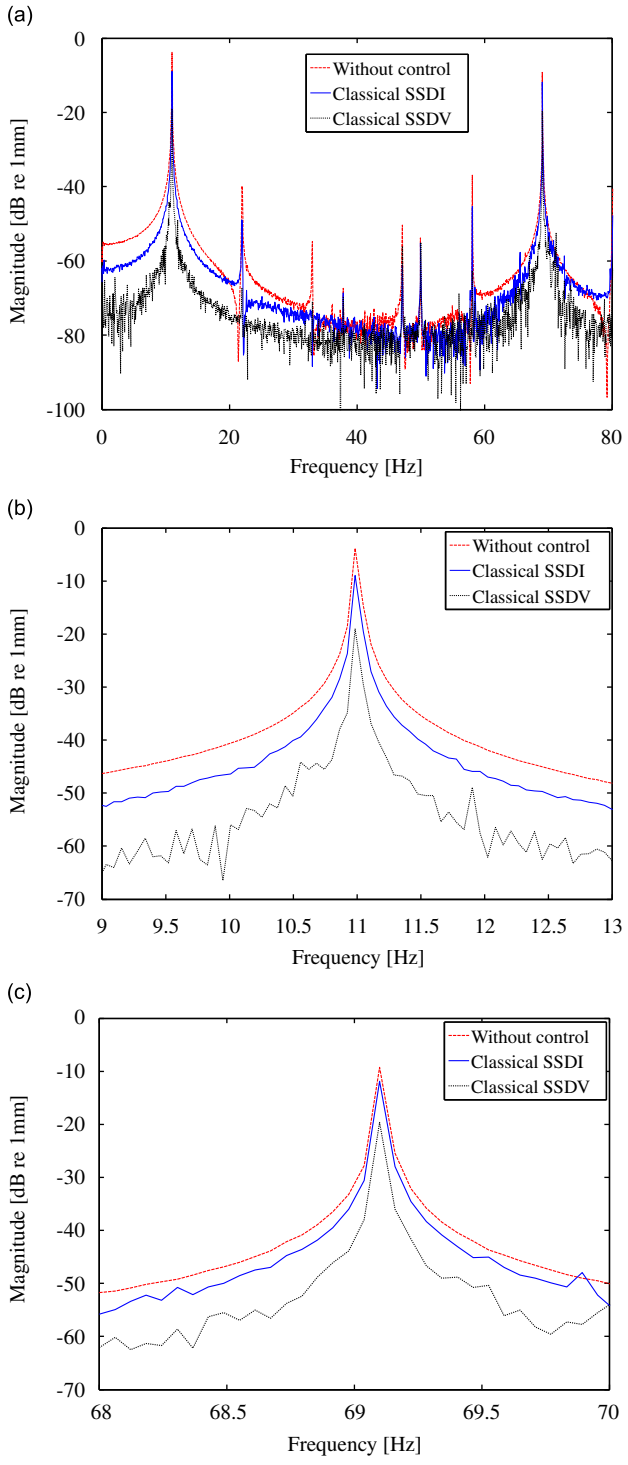

Fig. 9. Frequency of the displacement with the classical SSDI and classical SSDV techniques in two-mode control: (a) frequency response of the displacement; (b) enlarged around the resonant frequency of the first mode; and (c) enlarged around the resonant frequency of the second mode.

the normalized displacement are expressed in decibel as follows:

$$\text{The decibel value} = 20\log_{10}(\mathcal{F}(u/u_R))$$

where $\mathcal{F}$ is the symbol of Fourier Transformation and u_R is the reference displacement for normalization. The value of u_R is set to 1 mm in the following sections so that 0 dB is equivalent to 1 mm and -20 dB is equivalent to 0.1 mm.

5.1. Results of the single-mode control

In the single-mode control, only one mode is excited. Both the SSDI and SSDV techniques are used. Results are shown in Figs. 7 and 8. The first mode is reduced by 6 dB with classical SSDI and by 26.6 dB with classical SSDV. Damping effects of 2.9 and 19 dB are achieved respectively with classical SSDI and classical SSDV for the second mode. The control effects of both the SSDI and SSDV for the second mode are much lower than those for the first mode. This is due to the switch delay and the time needed for voltage inversion. The influence of the switch delay and the time for voltage inversion on control performance depends on the ratio of the switch delay or the inversion time to the vibration period. The greater the ratio is, the greater the influence is. The phase delay can be expressed as $\varphi_i = 2\pi\tau/\overline{T}_i$, where τ is the time delay and $\overline{T}_i$ is the period of the ith mode. As the frequency increases, the period decreases. This means that for the same time delay, the phase delay is larger for the high-order modes than for the low-order modes. Hence the influence of the switch delay and the inversion time is greater for high-order modes than for low-order modes. The performances of the classical SSDI and SSDV in single-mode control are summarized in Table 3. The decibel values of the first and second resonance peaks without and with control, and the damping effect, which is the reduction of peak values, are listed in the table.

5.2. Results of the two-mode control using the classical SSDI and SSDV

Next the classical SSDI and SSDV are used in the two-mode control. In the classical SSDI and SSDV, the voltage is inverted at each extremum. The beam is excited at the resonant frequencies of the first and second natural modes. The frequency response of the uncontrolled and controlled vibration of the beam is shown in Fig. 9. With the classical SSDI the

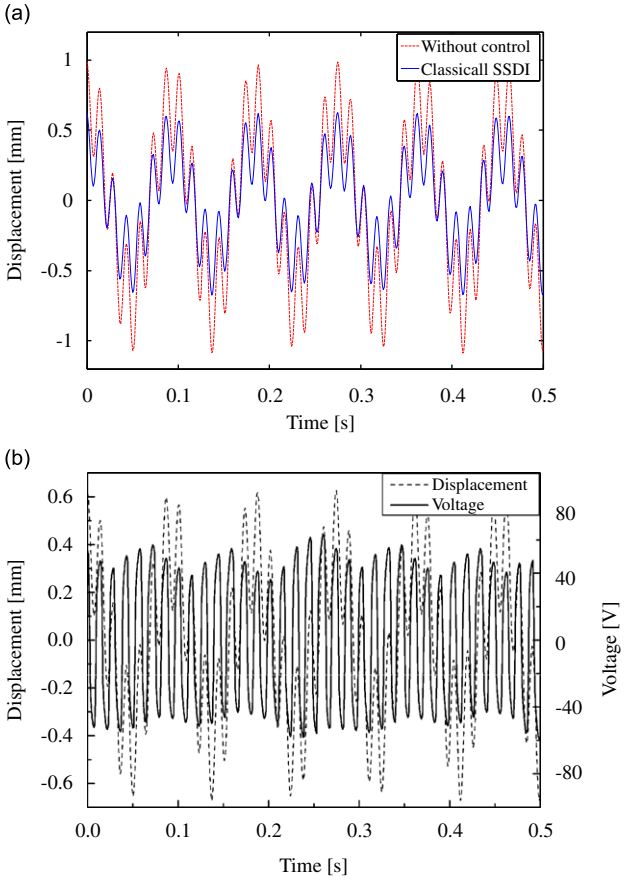

Fig. 10. Time response of the displacement and switched voltage with classical SSDI technique: (a) displacements with and without control and (b) switched voltage and controlled displacement.

vibration amplitude is reduced by 5.1 dB at the first resonant frequency and by 2.6 dB at the second resonant frequencies. The damping effects of the classical SSDI in the two-mode control are slightly smaller than those in the single-mode control. Fig. 10(a) shows the time response of the displacement before and after control and Fig. 10(b) shows the switched voltage. On average the voltage V_{sw} is about 40 V and the voltage V_{st} is about 10 V.

With the classical SSDV, the vibration amplitude is reduced by 15.2 dB at the first resonant frequency and by 10.4 dB at the second resonant frequencies, which are much smaller than those in single-mode control. Fig. 11(a) shows the time response of the displacement before and after control and Fig. 11(b) shows the switched voltage. The displacement with SSDV control is much smaller than that with SSDI control in Fig. 10. On average the voltage V_{sw} is about 70 V and the voltage V_{st} is about 4 V. The performances of the classical SSDI and SSDV in two-mode control are summarized in Table 4. The decibel values of the first and second resonance peaks without and with control, and the damping effect of the different control approaches, which is the reduction of peak values after control, are listed in the table.

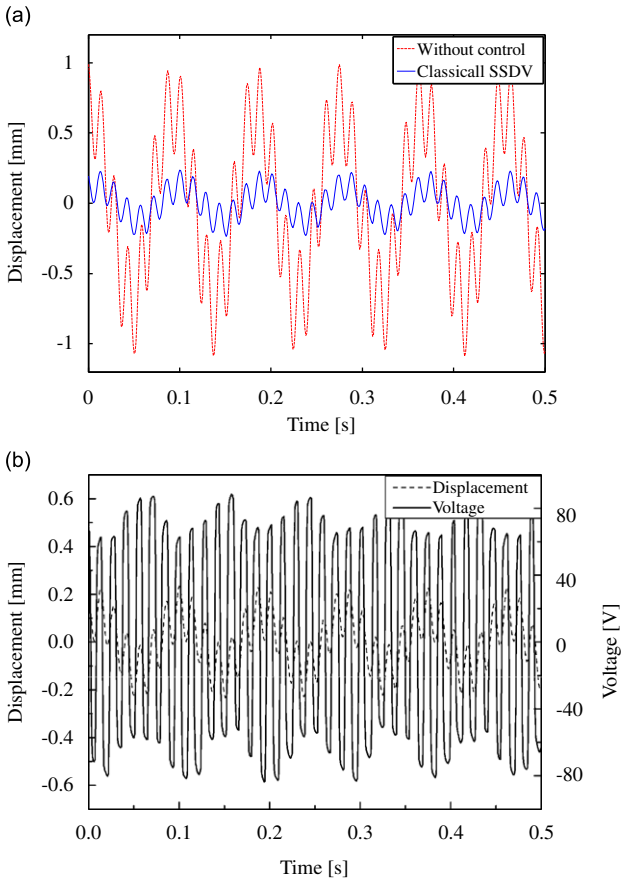

Fig. 11. Time response of the displacement and switched voltage with classical SSDV technique: (a) displacements with and without control and (b) switched voltage and controlled displacement.

Table 4
The control performances of different approaches in multimodal control.

Frequency (Hz)	Peak value without control (dB)	Peak value (upper) and reduction (lower) with classical SSDI (dB)	Peak value (upper) and reduction (lower) with classical SSDV (dB)	Peak value (upper) and reduction (lower) with SSDI based on energy (dB)	Peak value (upper) and reduction (lower) with adaptive SSDV based on energy (dB)
11	−3.8	−8.9	−19	−30.8	−29.9
		−5.1	−15.2	−27	−26.1
69.1	−9.2	−11.8	−19.6	−10.7	−20
		−2.6	−10.4	−1.5	−10.8

The deterioration of damping effect can be attributed to the shift of switching points which are influenced by the displacement of both the first and second modes in the two-mode control. The best damping effect is achieved for a given mode only when the voltage is inverted at each extremum of this mode. Hence, normally single-mode control gives the best control performance. However in two-mode control, the displacement is summation of the displacements of the two-mode as shown in Fig. 5 and the extrema of the composite displacement are neither the extrema of the first mode nor those of the second mode. Hence damping effect deteriorates for both modes in two-mode control.

The deterioration of damping effect is much smaller in SSDI than in SSDV. This can be attributed to the coupling effect of the voltage on the piezoelectric patch between the two modes. As shown in Eq. (25), the switched voltage is a function of the average effective displacement, which is affected by the vibration displacement of both modes as shown in Eq. (21). Since both modes contribute to the voltage on the piezoelectric patch, the voltage is higher in two-mode control than in single-mode control under the condition of the same displacement amplitude. Hence, the effect by the shift of the switching points is partially cancelled by the contribution of the other mode on the voltage. In SSDV, the voltage is mainly affected by the voltage source so that the contribution of the other mode on the voltage is negligible. Hence the effect by the shift of the switching points reflected in the control performance.

5.3. *Results of the two-mode control using the new switch control strategy*

5.3.1. *Results of SSDI*

First the new switch control strategy is combined with the SSDI technique and used in the two-mode control of the composite beam. The frequency response of displacement is shown in Fig. 12 and its time response is shown in Fig. 13(a).

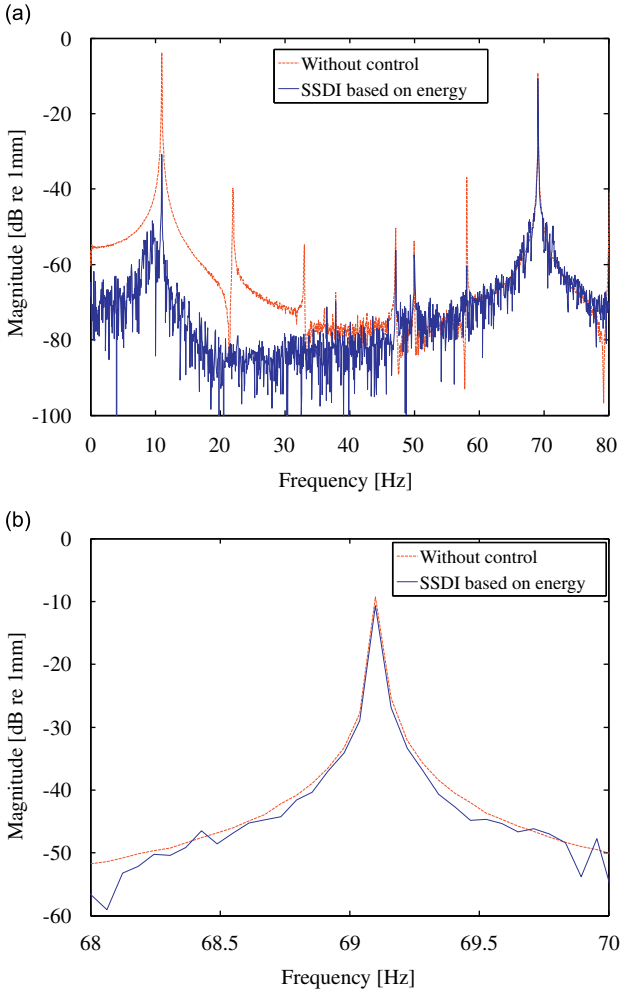

Fig. 12. Control performance of the improved SSDI technique with the new switch control strategy in two-mode control: (a) frequency response of the displacement and (b) enlarged around the resonant frequency of the second mode.

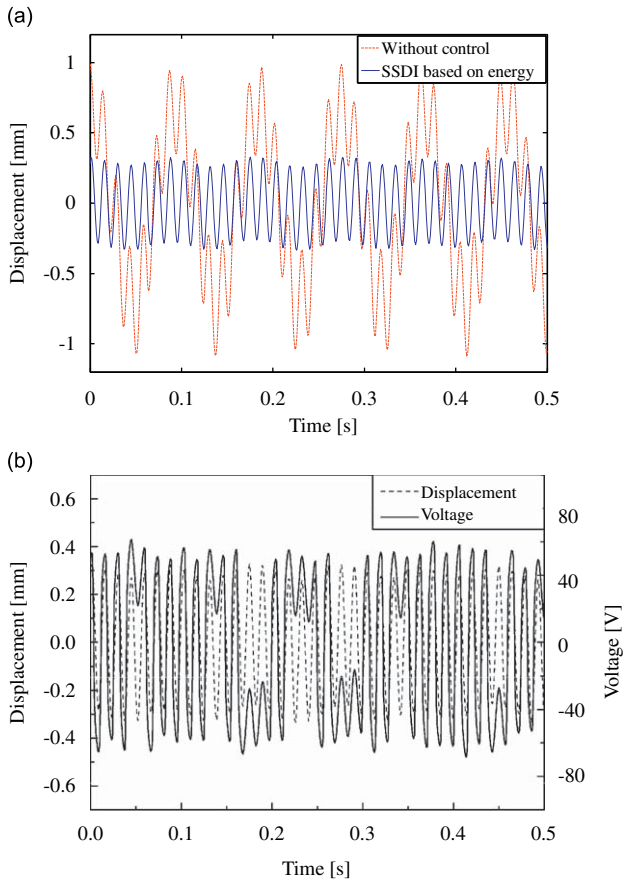

Fig. 13. Time response of the displacement and switched voltage using the improved SSDI technique with the new switch control strategy in two-mode control: (a) displacements with and without control and (b) switched voltage and controlled displacement.

The amplitude of the two modes is reduced by 27 and 1.5 dB, respectively. Fig. 13(a) also shows that the amplitude of the first mode is much smaller than that of the second mode. Compared to the two-mode control using the classical SSDI, the damping effect of the first mode is much higher, but that of the second mode is slightly lower. Comparing the controlled displacement in Figs. 13(a) and 10(a), the amplitude of the synthetic vibration of the first and second modes has been reduced by using the new switch control strategy. This means that the new method is effective in improving the global control performance.

Although the global control performance is improved by the new method, mixed control effects are achieved for different mode. This can be explained by the voltage signal. The switched voltage on the piezoelectric patch is shown in Fig. 13(b). It can be seen that voltage inversion does not occur at some of the displacement extrema. Skipping some extrema can increase the damping effect of the first mode, but decrease that of the second mode. The control performance of the first mode with the new method is even better than that in the single-mode control. This can be attributed to the coupling voltage generated by the first and second mode in two-mode control. In the single-mode control of the first mode, the voltage is generated by the first mode itself. The existence of the second-mode vibration leads to higher voltage in two-mode control than in single-mode control. Due to the better switch control algorithm, the voltage is efficiently utilized in the damping of the first mode. Hence, the damping effect of the first mode with the new method in two-mode control is better than that in single-mode control.

5.3.2. Results of SSDV with adaptive voltage source

Here the new switch control strategy is combined with the adaptive SSDV technique proposed in the former study [15] and used in the two-mode control of the composite beam. The output of the voltage source is very important for the control performance and stability of the system. The value of the voltage is adjusted adaptively by LMS-algorithm for optimal control performance in the adaptive SSDV. The frequency response of displacement is shown in Fig. 14 and its time response is shown in Fig. 15(a). The amplitude of the two modes is reduced by 26.1 and 10.8 dB, respectively. The damping effect of the second mode is almost the same as that using the classical SSDV, but damping effect of the first mode has been

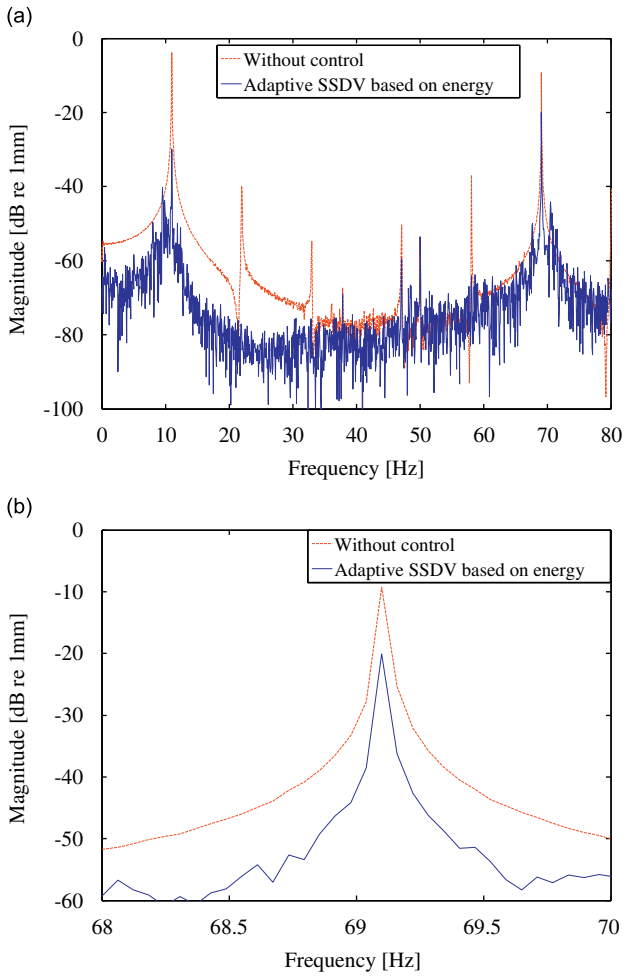

Fig. 14. Control performance of the improved SSDV technique with the new switch control strategy in two-mode control: (a) frequency response of the displacement and (b) enlarged around the resonant frequency of the second mode.

improved significantly. The amplitude of the synthetic vibration with control in Fig. 15(a) is much smaller than that in Fig. 11(a). This means that the new method with the combination of the new switch control strategy and the adaptive SSDV technique is a promising approach for the control of two-mode vibration of the beam.

The switched voltage on the piezoelectric patch is shown in Fig. 15(b). Similar to SSDI control with the new switch control strategy shown in Fig. 13(b), voltage inversion is prevented at some of the displacement extrema, but at a lower frequency. Skipping some extrema increases the damping effect of the first mode, but due to the lower skipping frequency damping effect of the second mode is barely affected.

The damping effects of all the control approaches in multimodal control are summarized in Table 4. The new switch control strategy exhibits better global control performance than the classical switching method in SSDI control. The combination of the new switch control strategy with the adaptive SSDV gives the best control performance in all considered methods.

6. Conclusions

In this study, a new switch control strategy based on an energy threshold is proposed for the synchronized switch damping techniques in multimode control. This strategy is derived from the total converted energy of a SSD system in a given time window. The new switch control strategy is used in both the SSDI technique and the SSDV technique, which are applied to the two-mode control of a composite beam. Their control performances are compared with those of the single-mode control and those of classical SSDI and SSDV techniques in two-mode control. The experimental results show that voltage inversion is prevented at some of the displacement extrema to increase the total converted energy. The

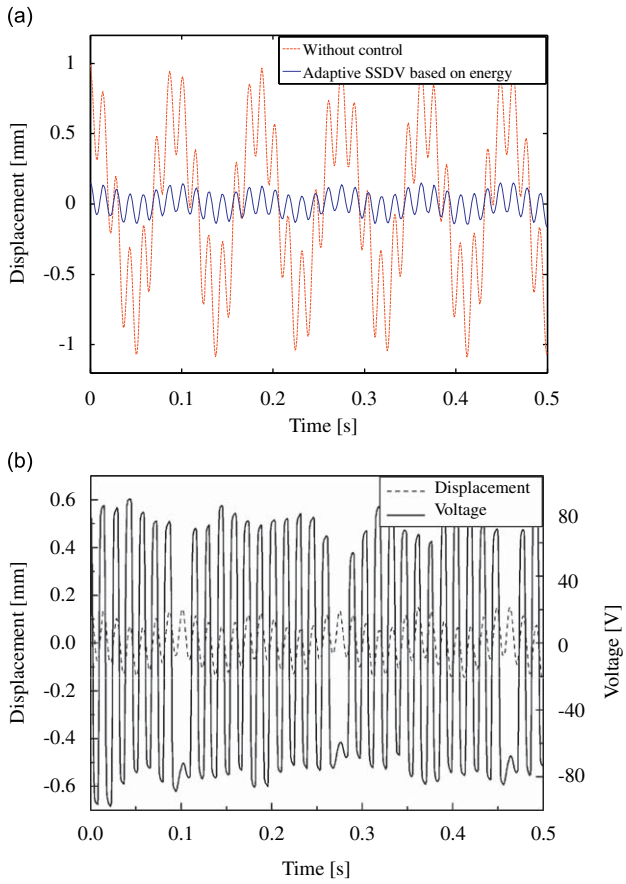

Fig. 15. Time response of the displacement and switched voltage using the improved SSDV technique with the new switch control strategy in two-mode control: (a) displacements with and without control and (b) switched voltage and controlled displacement.

improved SSDI using the new switch control strategy exhibits better overall damping effect in the resultant displacement than classical SSDI, which switches the voltage at every extremum. The improved SSDI is especially effective for the first mode of the beam. The damping effect of the improved SSDV using an adaptive voltage source and the new switch control strategy is also much better than that of the classical SSDV.

Acknowledgements

This research is supported by the National Natural Science Foundation of China under Grant 50775110, Aeronautical Science Fund under Grant 20091552017, NUAA Fund for Graduates Innovation under Grant BCXJ08-04, and Graduate Innovation Program of Jiangsu Province under Grant CX08B_048Z.

References

[1] S. Behrens, S.O.R. Moheimani, A.J. Fleming, Multiple mode current flowing passive piezoelectric shunt controller, *Journal of Sound and Vibration* 266 (2003) 929–942.
[2] D. Niederberger, A. Fleming, S.O.R. Moheimani, M. Morari, Adaptive multi-mode resonant piezoelectric shunt damping, *Smart Materials and Structures* 13 (2004) 1025–1035.
[3] M.A. Trindade, A. Benjeddou, R. Ohayon, Piezoelectric active vibration control of damped sandwich beams, *Journal of Sound and Vibration* 246 (2001) 653–677.
[4] L.R. Corr, W.W. Clark, Comparison of low-frequency piezoelectric switching shunt techniques for structural damping, *IOP Smart Materials and Structures* 11 (2002) 370–376.
[5] A.J. Fleming, S.O.R. Moheimani, Adaptive piezoelectric shunt damping, *IOP Smart Materials and Structures* 12 (2003) 36–48.
[6] M.S. Tsai, K.W. Wang, On the structural damping characteristics of active piezoelectric actuators with passive shunt, *Journal of Sound and Vibration* 221 (1999) 1–22.
[7] K. Makihara, J. Onoda, T. Yabu, Observability of self-sensing system using extended Kalman filter, *AIAA Journal* 45 (2007) 306–308.
[8] D. Guyomar, C. Richard, L. Petit, Non-linear system for vibration damping, *142th Meeting of Acoustical Society of America*, Fort Lauderdale, USA, 2001.
[9] C. Richard, D. Guyomar, D. Audigier, H. Bassaler, Enhanced semi-passive damping using continuous switching of a piezoelectric device on an inductor, *Proceedings of the SPIE International Symposium on Smart Structures and Materials: Damping and Isolation*, Vol. 3989, 2000, pp. 288–299.

[10] W.W. Clark, Vibration control with state-switching piezoelectric materials, *Journal of Intelligent Material Systems and Structures* 11 (2000) 263–271.
[11] A. Faiz, D. Guyomar, L. Petit, C. Buttay, Wave transmission reduction by a piezoelectric semi-passive technique, *Sensors and Actuators* 128 (2006) 230–237.
[12] A. Badel, G. Sebald, D. Guyomar, M. Lallart, E. Lefeuvre, C. Richard, J. Qiu, Piezoelectric vibration control by synchronized switching on adaptive voltage sources: towards wideband semi-active damping, *Journal of Acoustics Society of America* 119 (2006) 2815–2825.
[13] L.R. Corr, W.W. Clark, A novel semi-active multi-modal vibration control law for a piezoceramic actuator, *Journal of Vibration and Acoustics, Transactions of the ASME* 125 (2003) 214–222.
[14] D. Niederberger, Design of Optimal Autonomous Switching Circuits to Suppress Mechanical Vibration, *Lecture Notes in Computer Science*, Vol. 3414, Springer, 2005, pp. 511–525.
[15] D. Guyomar, A. Badel, Non-linear semi-passive multi-modal vibration damping: an efficient probabilistic approach, *Journal of Sound and Vibration* 294 (2006) 249–268.
[16] D. Guyomar, C. Richard, S. Mohammadi, Semi-passive random vibration control based on statistics, *Journal of Sound and Vibration* 307 (2007) 818–833.
[17] H.L. Ji, J.H. Qiu, A. Badel, Y.S. Chen, K.J. Zhu, Multimodal vibration control using a synchronized switch based on a displacement switching threshold, *Smart Materials and Structures* 18 (2009) 1–8.
[18] H.L. Ji, J.H. Qiu, A. Badel, Y.S. Chen, K.J. Zhu, Semi-active vibration control of a composite beam by adaptive synchronized switching on voltage sources based on LMS algorithm, *Journal of Intelligent Material Systems and Structures* 20 (2009) 939–947.